



CHORUS

This is the accepted manuscript made available via CHORUS. The article has been published as:

Discontinuity in the transport of strongly correlated two-dimensional hole systems in zero magnetic field

Jian Huang, L. N. Pfeiffer, and K. W. West

Phys. Rev. B **101**, 161110 — Published 20 April 2020

DOI: [10.1103/PhysRevB.101.161110](https://doi.org/10.1103/PhysRevB.101.161110)

Discontinuity in the transport of strongly correlated two-dimensional hole systems in zero magnetic field

Jian Huang

Department of Physics and Astronomy, Wayne State University, Detroit, MI 48201, USA

L. N. Pfeiffer and K. W. West

Department of Electrical Engineering, Princeton University, Princeton, NJ 08544

(Dated: March 18, 2020)

Adopting undoped ultra-clean two-dimensional hole systems, we approach a strongly correlated limit by reducing the carrier density down to $1 \times 10^9 \text{ cm}^{-2}$. The temperature dependence of the resistivity as a function of the carrier density reveals a characteristic energy scale displaying a benchmark critical behavior near a critical density of $p_c \sim 4 \times 10^9 \text{ cm}^{-2}$. The insulating state below p_c exhibits a sharp resistance discontinuity in response to heating across a critical temperature $T_{c1} \sim 30\text{mK}$, consistent with a first order transition. The dc response also identifies a second critical temperature T_{c2} where linear IV behavior is recovered. Similar effects are also demonstrated by varying an external electric field. The results support a complex quantum phase transition with intermediate phases.

The behaviors of electrons in solids are profoundly influenced by electron-electron interaction. The strongly correlated regime draws special interest because the correlation can fundamentally modify the system by giving rise to remarkable manybody effects even to the point of driving quantum phase transitions (QPTs). Effects associated with such QPTs are fundamental to expanding frontiers in areas such as Wigner crystal (WC) [1], magnetism, nonconventional superconductivity, and topological matters. QPTs in two-dimensional (2D) systems are anticipated to be complicated because the restricted quasi-long range order and the associated symmetry breaking [2, 3] that tend to drive a complex phase diagram. For example, melting transition via a correlated intermediate phase has been predicted for the classical case [4–9]. Experimental results in the degenerate limit [10–19] are so far insufficient for making identifications of clear signatures accompanying a phase transition, even though claims of liquid-solid transition involving WCs were made [11, 15, 18, 19]. This study focuses on the transport response in the strongly correlated 2D systems in an ultra-low disorder limit. The evidence of a phase transition is presented through both critical behaviors and sharp resistance discontinuities.

In correlated systems, effects stemming from disorders often complicate the situation through disorder localization [20]. Nevertheless, Anderson insulators differ from insulators caused by interaction (i.e. pinned WC cases). Interaction effect, reflected by $r_s = m^* e^2 / \epsilon \hbar^2 \sqrt{\pi p}$, becomes prominent only at low charge densities p . Take the WC for example, the anticipated $r_s \geq 37$ [21] corresponds to ultra-dilute p , i.e. $\leq 5 \times 10^9 \text{ cm}^{-2}$ for GaAs 2D holes (or $\leq 8 \times 10^8 \text{ cm}^{-2}$ for electrons). The effective mass m^* is $\sim 0.3 - 0.35$ [22, 23]. Localization easily occurs as the corresponding Fermi energy $E_F = n\pi\hbar^2/m^* \leq 30\mu\text{eV}$ falls below the disorder potential $eV_{dis} \sim 0.1\text{meV}$. e is the electron charge and ϵ is the dielectric constant. In addition, disorder screening is weakened because the large average charge spacing $2a$,

where $a = 1/\sqrt{\pi p} \geq 100 \text{ nm}$, becomes comparable to the screening length. As a result, interaction effect is often overwhelmed. Experimental proofs of such a disorder localization, i.e. in the insulating side of the 2D metal-to-insulator transition (MIT) [24], is the variable range hopping (VRH) transport [25, 26] at finite temperatures T : $\sigma(T) = \sigma_0 \exp(-T^*/T)^{1/\gamma}$ ($\gamma = 2, 3$). T^* measures the difference to the mobility edge. The activated T dependence, however, distinguishes from a phase transition in which a discontinuity is anticipated [27].

The situation becomes more intriguing when disorder is further reduced and interaction is no longer a perturbation. Insulators other than the Anderson localization are found [28, 29]. Previous experimental findings, i.e. in relation to thermal melting [11, 15], mostly support a smooth transition or crossover without observing any singularity. Because the systems are often weak insulators [11] and the translational correlation length ξ is too small to support genuine long-range orders, the collective modes [18, 19] alone are insufficient to clear up ambiguity associated with possible intermediate phases. Though the disorder effects are not yet well understood, they certainly contribute to reducing the long-range orders, as well as lowering the critical temperature (T_m) for a melting transition [9, 27, 30]. Therefore, accessing strongly correlated effects depends critically on the suppression of the disorders as suggested by recent studies [9, 31].

Because doping is a major source of disorders in semiconductors, undoped 2D hole systems, in (100) GaAs/AlGaAs HIGFETs (heterojunction-insulated-gate field-effect-transistors), are adopted for this study to reduce disorders down to the background level of the crystal growth chamber. At the hetero-interface, accumulation of ultra-dilute 2D hole carriers down to $p = 6 \times 10^8 \text{ cm}^{-2}$ is realized [29, 32] by solely biasing a top metal gate $d \sim 700 \text{ nm}$ above the 2D plane. With $d \gg a$, the reduction of r_s by dipolar screening [33] is minimized. The sample contains $6 \text{ mm} \times 0.8 \text{ mm}$ Hallbars fabricated with a lithographic technique [34, 35]. p at each fixed gate

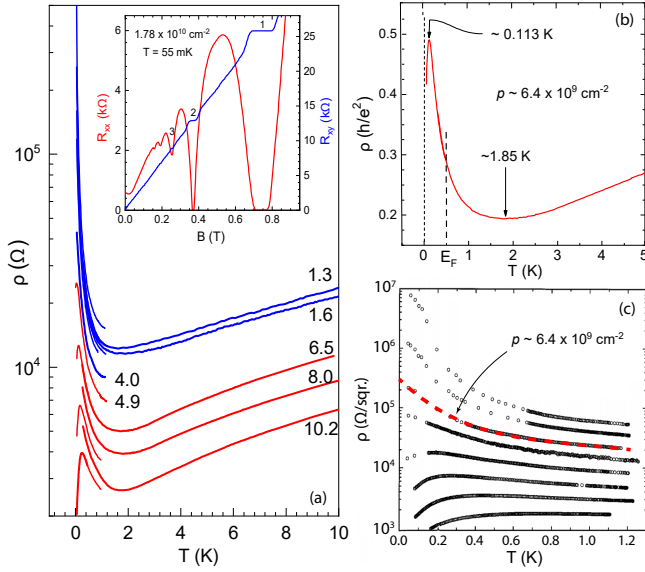


FIG. 1. T dependence of ρ for $p = 1.2, 1.5, 1.8, 2.3, 2.8, 4.0, 4.9, 6.4, 9.5,$ and $12.5 \times 10^9 \text{ cm}^{-2}$. Inset: Carrier density p is determined via the magnetoresistance and the Hall resistance. (b) $\rho(T)$ for $p = 6.4 \times 10^9 \text{ cm}^{-2}$. (c) $\rho(T)$ taken from Ref. [15] showing insulating behavior for $p = 6.4 \times 10^9 \text{ cm}^{-2}$.

bias is determined by the quantum Hall measurement. The inset of Fig.1(a) is for $p = 1.78 \times 10^{10} \text{ cm}^{-2}$.

The T dependence of the resistivity $\rho(T)$, measured with the four-probe ac lock-in technique, is shown in Fig. 1(a) for a number of p from 1.2 to $10.2 \times 10^9 \text{ cm}^{-2}$. The current excitation is maintained $\leq 1 \text{ nA}$ to avoid heating. The measurement was carried out in both a dilution refrigerator and a helium-3 cryostat to cover a temperature range from $\sim 0.02 \text{ K}$ to $\sim 10 \text{ K}$. $\rho(T)$ reaches a local minima (T_{min}) that varies from 1.6 to 1.8 K for the range of p . $\rho(T)$ rises, or $d\rho/dT < 0$, below T_{min} . Two different behaviors occur at lower T known as the signatures of the MIT: delocalization effect renders a metal-like state, with $d\rho/dT > 0$, for p greater than a critical value $p_c \sim 4 \times 10^9 \text{ cm}^{-2}$; while for $p < p_c$, ρ rises sharply with decreasing T .

We notice the p_c here is significantly lower than what is typically observed [15, 36]. A comparison is drawn with a previous study of doped p -type GaAs 2D systems of similar heterostructures [15]. For $p = 6.4 \times 10^9 \text{ cm}^{-2}$ (or $r_s \sim 30$) particularly, an insulator was found and interpreted as a WC phase in Ref. [15] [dotted red line in Fig 1(c)]. However, a metal state is observed here, as shown in Fig 1(b), with ρ well below h/e^2 . The reduction of disorder has clearly made the difference. We note that among nine different samples (from different wafers) tested, there is only a slight variation in $p_c = (4.3 \pm 0.3) \times 10^9 \text{ cm}^{-2}$.

As shown in Fig. 1(a), all metallic states start below a certain characteristic temperature, referred to as T_{max} since it is where $\rho(T)$ peaks, that varies with p . T_{max} is $\sim 113 \text{ mK}$ for $p = 6.4 \times 10^9 \text{ cm}^{-2}$ as shown by Fig. 1(b). T_{max} as a function of p is plotted in Fig. 2(a). The dashed

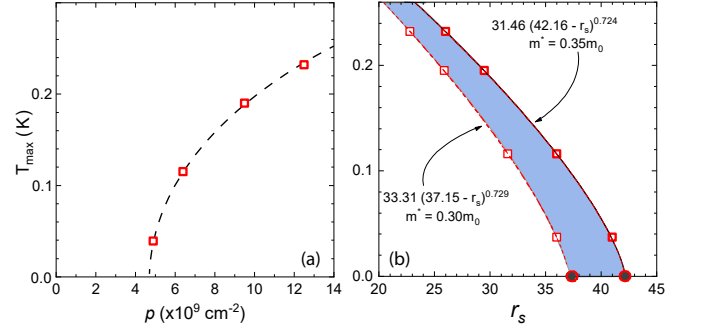


FIG. 2. (a) T_{max} vs. p . Dotted line represents a nonlinear fit to $A \cdot (p - p_c)^B$. (d) The result in (b) re-plotted as a function of r_s , with m^* taken between $0.3 - 0.35m_0$.

line is a nonlinear fit ($R^2 \approx 0.9997$) to $A \cdot \left(\frac{p-p_c}{p_c}\right)^\alpha$ with fitting parameters $A = 187.62 \pm 4.2$ and the exponent $\alpha = 0.46 \pm 0.05$. The abrupt collapse of T_{max} at p_c of $(4.62 \pm 0.04) \times 10^9 \text{ cm}^{-2}$ represents a benchmark critical behavior. Fig. 2(b) provides the corresponding r_s value which is approximately 40.

Note that r_s depends on the m^* , which is not precisely known in the dilute limit due to the influences of the band mass (involving band mixing of light and heavy hole bands) and the spin-orbit coupling [37]. Here, we simply provide a range (shaded region) for $m^* = 0.3 - 0.35m_0$ which produces a critical r_s between 37 and 42. This range is moderately higher than the predicted onset point of the WC based on quantum Monte Carlo simulations [21] without considering the disorder effects.

The insulating behavior for $p < p_c$ is compared with to Fig. 1(a) on double-logarithmic scales. Fig. 3(a) shows the conductivity $\sigma(T) = 1/\rho(T)$ for $p = 1.2 \times 10^9 \text{ cm}^{-2}$ for T from 1 K down to 30 mK . A non-activated power-law T dependence [29] is observed for $T \leq 300 \text{ mK}$. For a comparison, an activated behavior found in a more disordered sample is also plotted - $\sigma(T)$ plummets exponentially by more than five orders of magnitude for the same T range. The ac signal excitation for this measurement is 0.5 nA . The influences due to the level of the current excitation have not been adequately addressed.

Despite the large $r_s \sim 60 - 70$, the nonactivated $\sigma(T)$ shown in Fig. 3(a) exhibit no clear features reflecting a phase transition. On the contrary, the resistance, $\sim 500 \text{ k}\Omega$ at 30 mK , is low enough to support a strongly correlated liquid [29]. We first wondered whether this is related to the liquid reentrant behaviors at large r_s which have been considered for the gate screening effect which reduces the Coulomb interaction $e^2 p^{1/2}$ to dipolar interaction $e^2 d^2 p^{3/2}$. However, this is ruled out by the below dc results which verify a critical behavior in response to the change in signal excitation.

For $p \sim 3 \times 10^9 \text{ cm}^{-2}$, ρ is measured at various T with a dc-IV technique. Adopting $f\text{A}$ low noise source and an electrometer preamp with an input impedance of $10^{15} \Omega$, $\rho(T)$ is measured at various fixed current drives

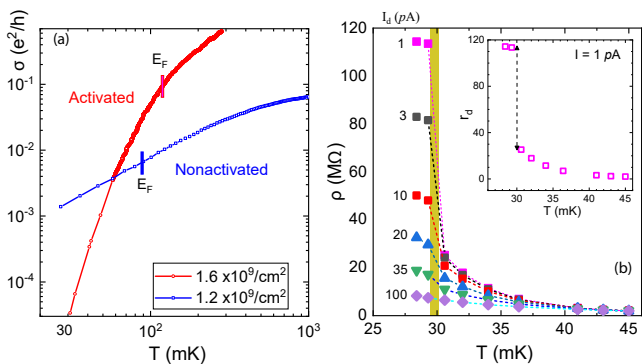


FIG. 3. (a) $\ln \sigma(T)$ vs. $\ln T$ for $p = 1.2 \times 10^9 \text{ cm}^{-2}$ in comparison to an activated behavior for $p = 1.6 \times 10^9 \text{ cm}^{-2}$. (b) $\rho(T)$ measured with different I_d . Dotted lines are a guide to the eye. The shaded region marks a sharp jump in ρ . Inset: discontinuity in the differential resistance r_d vs. T .

(I_d): 1, 3, 10, 20, 35, and 100 pA. As shown in Fig. 3(b), when $I_d = 100 \text{ pA}$ is applied, $\rho(T)$ recovers the power-law, consistent with the ac results. However, when $I_d = 35 \text{ pA}$ is used, a jump appears around 30 mK (shaded region), and it becomes increasingly stronger when less I_d is used.

For $I_d \leq 3 \text{ pA}$, $\rho(T)$ becomes piece-wise and a discontinuity appears via a jump of $\sim 65 \text{ M}\Omega$ over less than 2 mK of temperature change. The inset shows the differential resistance dV/dI as a function of T measured with 1 pA drive. Discontinuity in general is a signature of first-order phase transitions occurring across the phase boundaries. These insulating states are further examined with the dc measurement shown later. The location of the discontinuity is approximately $T \sim 30 \text{ mK}$ which is referred to as the critical temperature T_{c1} . Current induced heating is definitely ruled out because of the discontinuity. It is worth noting that below T_{c1} the resistance is extremely sensitive to the change in the drive up to 20 pA. The tiny current requirement, $\leq 3 \text{ pA}$, for observing discontinuity indicates that there is a critical excitation level above which the system is modified. Within the critical excitation, the T dependence at $T < T_{c1}$, is slight, $\sim 1 \text{ M}\Omega$ per mK, compared to the discontinuity.

On the other hand, the $\rho(T)$ behavior above T_{c1} draws a contrast because the I_d dependence significantly weakens and is eventually washed out above 43 mK. The T dependence follows a general power-law, distinct from the $T < T_{c1}$ scenario. $T = 43 \text{ mK}$ is referred to as T_{c2} . As shown below, T_{c2} actually marks a qualitative change in the dc-IV response.

Nonlinear dc-IV is performed for $p \sim 3 \times 10^9 \text{ cm}^{-2}$ at various T . The technique is well known for studying the pinned charge density waves (CDWs) [38]. Most previous studies with 2D semiconductor systems found weak insulators [11, 15] in contrast to the pinned CDWs. Our dc-IV results are shown in Fig. 4. Fig. 4(a) shows the dc-IV obtained below T_{c1} , at 28 mK, for $p \sim 3 \times 10^9 \text{ cm}^{-2}$. The derivative shown in Fig. 4(b) captures an enormous sub-threshold differential resistance dV/dI up to $\sim 110 \text{ M}\Omega$, comparable to that of pinned CDWs. The current corresponding to the threshold voltage $V_{th} \sim 0.25 \text{ mV}$ is just

$\sim 2 - 3 \text{ pA}$. dV/dI plummets by two orders of magnitude when V exceeds V_{th} .

The sub-threshold resistance shown in Fig. 4(a) and (b) support a transport response primarily in the form of potential energy because of the negligible current ($\leq 1 \text{ pA}$). Because Anderson localization is excluded in our case, we consider the pinning scenario. Setting eV_{th} equal to the sum of all the single particle potential energy $\epsilon = eV_{th}/L$, the average particle displacement l (from the equilibrium) is found to be $\sim 0.13a$ where $a = 1/\sqrt{\pi p} \sim 100 \text{ nm}$. $L \sim 1 \text{ mm}$ is the distance over which the electric field is applied. ϵ is approximately 3.5 neV which is approximately 10^{-3} of $k_B T_{c1}$ and 4×10^{-6} of the Coulomb energy E_c .

Because a true long range order is prohibited in 2D [2], we consider quasi-long range correlation length ξ . For the cases of charge pinning, ξ scales with dV/dI up to V_{th} and can be estimated at V_{th} by balancing the total potential energy $N\epsilon$ and the pinning energy $-(1/2)\kappa a$ [11, 12]. $\kappa = 0.245e^2 p^{3/2}/4\pi\epsilon_0\epsilon$ is the shear modulus and $N = p\xi^2$ is the particle numbers within a single domain. Utilizing the average particle displacement l found earlier, N is estimated as $\sim 10^5$ which corresponds to a $\xi \geq 50 \mu\text{m}$.

Fig. 4(c) shows how the IV behavior evolves in response to the increase of T . At $T = 32 \text{ mK}$, the sub-threshold dV/dI drops substantially to $\sim 10 \text{ M}\Omega$, nearly one tenth of that measured at 28 mK, even though a softer non-linearity is retained. The measured current rises rapidly around $V = 0.15 \text{ mV}$. The nonlinear IV diminishes upon reaching $T \geq T_{c2}$. The recovery of the linear behavior is consistent with previous reports [11, 12, 15] interpreted as the onset of an isotropic liquid. Note that the linear behavior should not be confused with a metal since the differential resistance remains approximately $2 \text{ M}\Omega$ well beyond h/e^2 . Viscous flow in strongly correlated liquids is a likely candidate and relevant theoretical work can be found in Ref. [39]. It is worth noting that the differential resistance, which measures the dynamical response, acquires approximately the same value for all three temperatures when the current drive is beyond 25 pA. The value of the differential resistance at this point agrees with the resistance under a thermal effect above 40 mK shown in Fig. 3(b). It therefore indicates that increasing

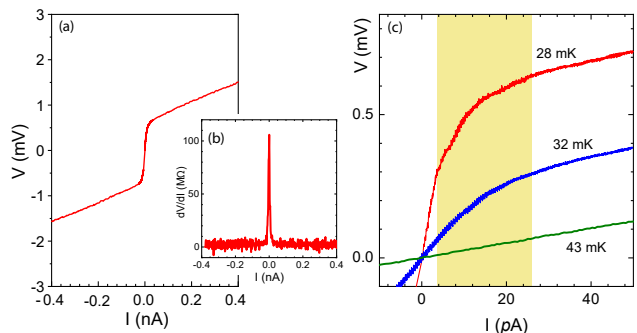


FIG. 4. (a) dc-IV measured for $p \sim 3 \times 10^9 \text{ cm}^{-2}$ (or $r_s \sim 50$) and (b) shows the derivative dV/dI . (c) Comparison of dc-IV behaviors obtained at $T = 28, 32$ and 43 mK . (d) dc-IV for $p > p_c$. Inset: the same plot on same scales as (c).

the electric field results in similar changes to the electron states, even though it does not produce a discontinuity as observed in the thermally-driven case.

Based on the results shown in both Fig. 3 and Fig. 4, it is clear the discontinuity at T_{c1} separates a strong and a weak insulator. Both insulators distinguish from the unpinned situation above T_{c2} . Therefore, an intermediate state between T_{c1} and T_{c2} is supported. Nevertheless, the relevance to the theories on classical melting is yet to be confirmed because transitions involving Hexatics [4–7, 9], stripes/bubbles, and microemulsions [8] are expected to be second order.

A parallelism appears between the thermal and electric effects. There is a critical excitation where a threshold of current is triggered. Meanwhile, there is second critical excitation at higher value above which the systems attains the same dynamic response of an isotropic liquid, independent of T . The intermediate state is shown as the shaded region in Fig. 4(c).

The dc-IV response is drastically altered if the carrier density is above $p_c \sim 4.6 \times 10^9 \text{ cm}^{-2}$. The dc-IV behavior obtained at similar T shown in Fig. 4(d) is for $5 \times 10^9 \text{ cm}^{-2}$ which is just slightly above p_c . Thresh-

old behavior diminishes completely and the differential resistance plummets to $1/20,000$ of that for $3 \times 10^9 \text{ cm}^{-2}$ [Fig. 4(a)]. The inset is the same plot shown on the same scales of Fig. 4(c) which indicates remarkable suppression of the resistance across p_c . Therefore, it provides further support to the critical behavior shown in Fig. 2(a) as an indication of a phase transition driven by increasing interaction near a critical point of $r_s \sim 40$.

The key findings of this study in terms of the discontinuity in the thermal effect and the critical behavior are absent in previous studies [11, 15]. We offer two possible explanations. 1. The signal excitation used in previous studies is beyond the critical electric field which is exceedingly small. 2. T_{c1} (T_{c2}) is approximately $1/4$ ($1/3$) of the classical melting point $E_c/127$ which can not be accounted for by quantum fluctuations alone [30]. The suppression of T_c by disorder has been recognized [9, 31] which could render the T_c beyond experimental reach.

The work at Wayne State University is supported by NSF under DMR-1410302, The work at Princeton University was funded by the Gordon and Betty Moore Foundation through the EPiQS initiative Grant GBMF4420, and by the National Science Foundation MRSEC Grant DMR 1420541.

-
- [1] E. Wigner, Phys. Rev. **46**, 1002 (1934).
 [2] N. D. Mermin, Phys. Rev. **176**, 250 (1968).
 [3] J. M. Kosterlitz, Journal of Physics C: Solid State Physics **7**, 1046 (1974).
 [4] B. I. Halperin and D. R. Nelson, Phys. Rev. Lett. **41**, 121 (1978).
 [5] D. R. Nelson and B. I. Halperin, Phys. Rev. B **19**, 2457 (1979).
 [6] D. R. Nelson and B. I. Halperin, Phys. Rev. B **21**, 5312 (1980).
 [7] A. P. Young, Phys. Rev. B **19**, 1855 (1979).
 [8] B. Spivak and S. A. Kivelson, Physical Review B **70**, 155114 (2004).
 [9] B. K. Clark, M. Casula, and D. M. Ceperley, Phys. Rev. Lett. **103**, 055701 (2009).
 [10] H. W. Jiang, H. L. Stormer, D. C. Tsui, L. N. Pfeiffer, and K. W. West, Phys. Rev. B **44**, 8107 (1991).
 [11] V. J. Goldman, M. Santos, M. Shayegan, and J. E. Cunningham, Phys. Rev. Lett. **65**, 2189 (1990).
 [12] F. I. B. Williams, P. A. Wright, R. G. Clark, E. Y. Andrei, G. Deville, D. C. Glatli, O. Probst, B. Etienne, C. Dorin, C. T. Foxon, and J. J. Harris, Phys. Rev. Lett. **66**, 3285 (1991).
 [13] S. V. Kravchenko, J. A. A. J. Perenboom, and V. M. Pudalov, Phys. Rev. B **44**, 13513 (1991).
 [14] V. M. Pudalov, M. D'Iorio, S. V. Kravchenko, and J. W. Campbell, Phys. Rev. Lett. **70**, 1866 (1993).
 [15] J. Yoon, C. C. Li, D. Shahar, D. C. Tsui, and M. Shayegan, Phys. Rev. Lett. **82**, 1744 (1999).
 [16] P. Brussarski, S. Li, S. Kravchenko, A. Shashkin, and M. Sarachik, arXiv preprint arXiv:1704.04479 (2017).
 [17] E. Y. Andrei, G. Deville, D. C. Glatli, F. I. B. Williams, E. Paris, and B. Etienne, Phys. Rev. Lett. **60**, 2765 (1988).
 [18] Y. P. Chen, G. Sambandamurthy, Z. Wang, R. Lewis, L. Engel, D. Tsui, P. Ye, L. Pfeiffer, and K. West, Nature Physics **2**, 452 (2006).
 [19] J. Jang, B. M. Hunt, L. N. Pfeiffer, K. W. West, and R. C. Ashoori, Nature Physics **13**, 340 (2017).
 [20] P. W. Anderson, Phys. Rev. **109**, 1492 (1958).
 [21] D. M. Ceperley and B. J. Alder, Phys. Rev. Lett. **45**, 566 (1980).
 [22] T. M. Lu, Z. F. Li, D. C. Tsui, M. J. Manfra, L. N. Pfeiffer, and K. W. West, Applied Physics Letters **92**, 012109 (2008), <http://dx.doi.org/10.1063/1.2830016>.
 [23] H. Zhu, K. Lai, D. Tsui, S. Bayrakci, N. Ong, M. Manfra, L. Pfeiffer, and K. West, Solid State Communications **141**, 510 (2007).
 [24] S. V. Kravchenko, G. V. Kravchenko, J. E. Furneaux, V. M. Pudalov, and M. D'Iorio, Phys. Rev. B **50**, 8039 (1994).
 [25] N. Mott, Journal of Non-Crystalline Solids **1**, 1 (1968).
 [26] B. I. Shklovskii and A. L. Efros, *Electronic properties of doped semiconductors*, Vol. 45 (Springer Science & Business Media, 2013).
 [27] K. J. Strandburg, Rev. Mod. Phys. **61**, 747 (1989).
 [28] H. Noh, M. P. Lilly, D. C. Tsui, J. A. Simmons, L. N. Pfeiffer, and K. W. West, Phys. Rev. B **68**, 241308 (2003).
 [29] J. Huang, D. S. Novikov, D. C. Tsui, L. N. Pfeiffer, and K. W. West, Phys. Rev. B **74**, 201302 (2006).
 [30] M. Imada and M. Takahashi, Journal of the Physical Society of Japan **53**, 3770 (1984).
 [31] T. Knighton, Z. Wu, J. Huang, A. Serafin, J. Xia, L. Pfeiffer, and K. West, Physical Review B **97**, 085135 (2018).

- [32] J. Huang, L. N. Pfeiffer, and K. W. West, *Phys. Rev. B* **85**, 041304 (2012).
- [33] B. Spivak, S. V. Kravchenko, S. A. Kivelson, and X. P. A. Gao, *Rev. Mod. Phys.* **82**, 1743 (2010).
- [34] B. E. Kane, L. N. Pfeiffer, and K. W. West, *Applied Physics Letters* **67**, 1262 (1995).
- [35] J. Huang, D. S. Novikov, D. C. Tsui, L. N. Pfeifer, and K. W. West, *International Journal of Modern Physics B* **21**, 1219 (2007).
- [36] M. Y. Simmons, A. R. Hamilton, M. Pepper, E. H. Linfield, P. D. Rose, D. A. Ritchie, A. K. Savchenko, and T. G. Griffiths, *Phys. Rev. Lett.* **80**, 1292 (1998).
- [37] E. Berg, M. S. Rudner, and S. A. Kivelson, *Phys. Rev. B* **85**, 035116 (2012).
- [38] G. Grüner, *Rev. Mod. Phys.* **60**, 1129 (1988).
- [39] A. V. Andreev, S. A. Kivelson, and B. Spivak, *Phys. Rev. Lett.* **106**, 256804 (2011).